

See discussions, stats, and author profiles for this publication at: <https://www.researchgate.net/publication/6418135>

Membrane “Lens” Effect: Focusing the Formation of Reactive Nitrogen Oxides from the • NO/O₂ Reaction

ARTICLE in CHEMICAL RESEARCH IN TOXICOLOGY · MAY 2007

Impact Factor: 3.53 · DOI: 10.1021/tx700010h · Source: PubMed

CITATIONS

50

READS

44

6 AUTHORS, INCLUDING:



Matias Moller

University of the Republic, Uruguay

23 PUBLICATIONS 492 CITATIONS

SEE PROFILE



John M Robinson

South Dakota State University

40 PUBLICATIONS 481 CITATIONS

SEE PROFILE



Jack Lancaster

University of Pittsburgh

167 PUBLICATIONS 11,725 CITATIONS

SEE PROFILE



Ana Denicola

University of the Republic, Uruguay

86 PUBLICATIONS 3,834 CITATIONS

SEE PROFILE

Membrane “Lens” Effect: Focusing the Formation of Reactive Nitrogen Oxides from the •NO/O₂ Reaction

Matias N. Möller,^{†,§} Qian Li,^{‡,§} Dario A. Vitturi,^{†,||} John M. Robinson,[‡]
Jack R. Lancaster, Jr.,[‡] and Ana Denicola^{*,†}

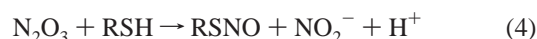
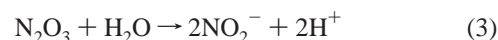
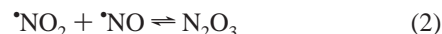
Laboratorio de Fisicoquímica Biológica, Facultad de Ciencias, and Center for Free Radical and Biomedical Research, Universidad de la República, Montevideo 11400, Uruguay, and Departments of Anesthesiology, Physiology & Biophysics, and Environmental Health Sciences, Center for Free Radical Biology, the University of Alabama at Birmingham, Birmingham, Alabama 35294

Received January 9, 2007

It was previously observed that lipid membranes accelerate •NO disappearance (Liu et al. (1998) *Proc. Natl. Acad. Sci. U.S.A.* 95, 2175), and here, we demonstrate that this translates into increased rates of •NO₂ production and nitrosative chemistry. Not only the phospholipid membranes but also the atherosclerosis-related low-density lipoprotein (LDL) were able to accelerate the formation of •NO₂, studied by stopped-flow spectrophotometry using ABTS as a probe. In addition, membranes, LDL, and Triton X-100 micelles significantly accelerated *S*-nitrosation of glutathione and captopril. It is shown here that autoxidation of •NO occurs 30 times more rapidly within the hydrophobic interior of these particles than in an equal volume of water, approximately 1 order of magnitude less than previous reports. This acceleration can be explained by the ~3 times higher solubility of •NO and O₂ into these hydrophobic phases relative to water, which results in a higher local concentration of reactants (“lens effect”) and, therefore, a higher rate of reaction. It is predicted that 50% of the oxidizing and nitrosating species derived from •NO autoxidation in cells will be formed in the small volume comprising cellular membranes (3% of the total); thus, biomolecules near the membranes will be exposed to fluxes of reactive nitrogen species 30-fold higher than their cytosolic counterparts.

Introduction

Nitric oxide (•NO¹, nitrogen monoxide), unlike other free radicals, is relatively stable, only reacting rapidly with other paramagnetic species such as other radicals (O₂•[−], LOO•, and GS•) and transition metal centers. The reaction between •NO and O₂, also termed autoxidation (eq 1), is particularly interesting because the products are potent oxidizing and especially nitrosating agents (1–4). Dinitrogen trioxide (N₂O₃), the intermediate that leads to nitrite after hydrolysis (eqs 2 and 3), is considered the major nitrosating agent in biological systems (eq 4, ref 5). Alternatively, thiols can be nitrosated through a radical mechanism involving the oxidation of thiol by nitrogen dioxide (•NO₂) to the thiyl radical, which then reacts with •NO to yield *S*-nitrosothiol (eqs 5 and 6, ref 6).



Biological *S*-nitrosation is a novel post-translational modification possibly involved in the regulation of cellular functions and disease (5, 7–12). Proposed roles for *S*-nitrosation include inhibition of platelet degranulation and aggregation (9) and regulation of apoptosis through glyceraldehyde-3-phosphate dehydrogenase modification (10) as well as involvement in the pathogenesis of Parkinson’s disease (11) and amyotrophic lateral sclerosis (12). In addition, the *N*-nitrosation of DNA bases can lead to their deamination and to mutagenicity (13), whereas the nitrosation of oxidized lipids could lead to the formation of potent bioactive nitrolipids (14, 15). Despite the potential biological relevance of nitrosation, the molecular mechanisms leading to nitrosation *in vivo* are not clear. At first, the autoxidation of •NO was considered too slow to be biologically relevant because the rate of this reaction depends on the square of •NO concentration, and physiological concentrations of •NO

* To whom correspondence should be addressed. Tel/Fax: (5982) 5250749. E-mail: denicola@fcien.edu.uy.

[†] Universidad de la República.

[‡] University of Alabama at Birmingham.

[§] Both authors contributed equally to this work.

^{||} Current address: Department of Pathology, University of Alabama at Birmingham, Birmingham, AL 35294.

¹ Abbreviations: •NO, nitric oxide, nitrogen monoxide; •NO₂, nitrogen dioxide; N₂O₃, dinitrogen trioxide; LDL, low-density lipoprotein; DLPC, dilauroyl phosphatidylcholine; EYPC, egg-yolk phosphatidylcholine; DTPA, diethylenetriaminepentaacetic acid; Proli/NO, prolinenonoate; *K*_p, partition coefficient; *C*_h, concentration of the hydrophobic phase; *v*_h, partial specific volume; *λ*, acceleration coefficient; ABTS, 2,2′-azino-bis(3-ethylbenzothiazoline-6-sulfonic acid); Cap, captopril; NEM, *N*-ethylmaleimide; RSNO, *S*-nitrosothiol.

are low (eq 7, $k = 3.0 \times 10^6 \text{ M}^{-2} \text{ s}^{-1}$, ref 1), but this perspective changed when Liu et al. showed that membranes accelerate $\cdot\text{NO}$ autoxidation (16) and has thereafter been considered a possible route of biological nitrosation (5, 7, 8, 14, 17).

$$-d[\cdot\text{NO}]/dt = 4k[\cdot\text{NO}]^2 [\text{O}_2] \quad (7)$$

Here, we demonstrate that not only $\cdot\text{NO}$ disappearance (16) but also $\cdot\text{NO}_2$ and *S*-nitrosothiol formation occur more rapidly in the presence of different hydrophobic phases, including phospholipid membranes, detergent micelles and low-density lipoprotein (LDL). In addition to its biomedical importance (18), LDL constitutes a good model to study the mechanism by which $\cdot\text{NO}$ autoxidation is accelerated because the solubility and the diffusion of $\cdot\text{NO}$ in LDL are well characterized (19, 20). Our results indicate that, under biological conditions, the limiting reaction in $\cdot\text{NO}$ autoxidation (eq 1) is accelerated 30 times within the hydrophobic phase, leading to a faster rate of oxidizing- and nitrosating-species formation, mainly due to the favored partitioning of $\cdot\text{NO}$ and O_2 in the hydrophobic core of lipoproteins and membranes.

Materials and Methods

Materials. $\cdot\text{NO}$ and N_2 were purchased from AGA SA (Montevideo, Uruguay). Dilauroyl phosphatidylcholine (DLPC) and egg-yolk phosphatidylcholine (EYPC) were from Avanti Polar Lipids (Pelham, AL), prolinenonoate (Proli/NO) was from Alexis Biochemicals (San Diego, CA). Glutathione (GSH), captopril (Cap), sulfanilamide, and all other reagents were of analytical grade and purchased from Sigma (Saint Louis, MO). LDL was purified by ultracentrifugation in a KBr gradient from the human plasma of healthy volunteers as reported previously (20). LDL protein concentration was determined at 280 nm ($\epsilon_{280} = 1.05 \text{ mg}^{-1} \text{ mL cm}^{-1}$, ref 20), and the hydrophobic phase concentration (C_h) was calculated considering that protein accounts for 22% of the particle weight (21), thus $C_h^{\text{LDL}} = C_{\text{prol}}/0.22$. For stopped-flow experiments, DLPC and EYPC liposomes were extruded 10 times through a 100 nm filter (Northern Lipids, Inc., Canada) to achieve a uniform unilamellar population of liposomes, which considerably improved their optical properties. Stock $\cdot\text{NO}$ solutions were prepared as done before in distilled water (19). Briefly, the system consisting of a 5 M NaOH trap and a gas collecting bottle was deoxygenated for 3 h with N_2 sparging and then switched to $\cdot\text{NO}$ gas for 15 min.

Polarographic Study of $\cdot\text{NO}$ Autoxidation. The disappearance of $\cdot\text{NO}$ was followed using an ISO-NO electrode (WPI, Inc. Sarasota, FL) after injecting Proli/NO to yield a final $\cdot\text{NO}$ concentration below 4 μM in a capped, well stirred, and thermostatted vessel with no headspace containing air-equilibrated phosphate buffer (5 mM sodium phosphate, 100 μM DTPA, pH 7.4, 240 μM O_2 , 25 $^\circ\text{C}$). The concentration of O_2 was well in excess of $[\cdot\text{NO}]$ ($[\text{O}_2] > 50 [\cdot\text{NO}]$) so that a second-order plot ($1/[\cdot\text{NO}]$ vs t) yields a slope equal to the observed rate constant $k_{\text{obs}} = 4k[\text{O}_2]$. The autoxidation of $\cdot\text{NO}$ was followed for at least two half-lives, not considering the initial 40 s (because of the response of the electrode). Proli/NO was prepared in 50 mM NaOH, and the concentration of $\cdot\text{NO}$ released was calibrated either with an excess of oxymyoglobin ($\epsilon_{582} = 0.0121 \text{ } \mu\text{M}^{-1} \text{ cm}^{-1}$ and $\epsilon_{545} = 0.0091 \text{ } \mu\text{M}^{-1} \text{ cm}^{-1}$) or using the $\cdot\text{NO}$ electrode calibrated as previously described (20). In control experiments, we confirmed that the presence of Triton X-100, DLPC membranes, and LDL does not affect the intrinsic response of the electrode to $\cdot\text{NO}$ (data not shown).

$\cdot\text{NO}$ Partition Coefficient Determination. The $\cdot\text{NO}$ partition coefficients (K_P^{NO}) were determined as previously described (20) using 40 mg/mL Triton X-100 or DLPC in 5 mM sodium phosphate and 100 μM DTPA at pH 7.4 and compared with the buffer alone. The measurements ($n = 4-6$) were performed at room temperature. Because the present work refers to the total volume of the particles,

with no assumption about what fraction of that volume is actually hydrophobic, previous partition coefficients (20) were corrected to exclude the hydrophobic fraction assumption (F_h ; see ref 20); therefore, $K_P^{\text{corr}} = (K_P - 1)F_h + 1$.

$\cdot\text{NO}_2$ Formation Studied by ABTS Oxidation. Nitrogen dioxide reacts rapidly with ABTS (2,2'-azino-bis(3-ethylbenzo-thiazoline-6-sulfonic acid)), $k = 2.2 \times 10^7 \text{ M}^{-1} \text{ s}^{-1}$ (22), to yield the stable radical $\text{ABTS}^{\cdot+}$ that can be followed spectrophotometrically at 660 nm ($\epsilon_{660} = 12.000 \text{ M}^{-1} \text{ cm}^{-1}$, ref 1). Experiments were performed on a Cary 50 Varian spectrophotometer coupled to a RX-2000 rapid kinetics accessory from Applied Photophysics. The stopped-flow accessory thermostatted jacket was deoxygenated using 10 mM dithionite dissolved in 50 mM Tris at pH 8.0 as suggested by the manufacturer. One syringe contained $\cdot\text{NO}$ (150 or 300 μM) diluted in deoxygenated water (boiled and N_2 -sparged for 2 h in a septum-sealed bottle), and the other syringe contained 2 mM ABTS in air-equilibrated phosphate buffer (3 mM, 0.1 mM DTPA, pH 7.4, 240 μM O_2 , 25 $^\circ\text{C}$) with or without the hydrophobic phase. Paired experiments were performed using the same $\cdot\text{NO}$ solution for experiments with and without the hydrophobic phase ($n = 10$ each). Radical $\text{ABTS}^{\cdot+}$ was prepared by reacting 7 mM ABTS with 3 mM ammonium persulfate for 12 h to ensure reaction completion. A 40-fold molar excess of $\text{ABTS}^{\cdot+}$ was used to block LDL-reducing groups. After 10–20 s, the remaining $\text{ABTS}^{\cdot+}$ was removed by gel filtration.

Modification of LDL Exposed to $\cdot\text{NO}/\text{O}_2$. LDL (1 μM) was treated with 500 μM $\cdot\text{NO}$ from Proli/NO in 10 mM phosphate, 100 μM DTPA at pH 7.4 for 30 min at 37 $^\circ\text{C}$ in a magnetically stirred capped vial with no headspace. α -Tocopherylquinone was quantified by HPLC as described previously (23). The formation of fluorescent lipoprotein adducts was studied by following changes in the emission spectrum ($\lambda_{\text{ex}} = 365 \text{ nm}$, $\lambda_{\text{em}} = 400-500 \text{ nm}$), as done previously (24), using an LS2 Aminco-Bowman spectrofluorimeter. The intrinsic LDL tryptophan fluorescence ($\lambda_{\text{ex}} = 295 \text{ nm}$, $\lambda_{\text{em}} = 330 \text{ nm}$) was used as a measure of its oxidative status. LDL *S*-nitrosation was studied as described below.

Nitrogen Oxide Products Measured by Chemiluminescence. Nitrogen oxide products including nitrite, nitrate, *S*-nitrosothiol, and Hg^{2+} -resistant products were measured by a well-validated chemiluminescence assay (25). These nitrogen oxide products except nitrate are stoichiometrically converted to $\cdot\text{NO}$ by acidic tri-iodide, and the liberated $\cdot\text{NO}$ is detected by its chemiluminescent reaction with ozone (25). The pretreatment of samples with nitrate reductase converts nitrate to nitrite, whereas the pretreatment with sulfanilamide eliminates nitrite, and the pretreatment with HgCl_2 eliminates nitrosothiols so that the content of each specific product is determined using differential treatments (25). All samples were prepared under rapid stirring in a capped vial (without headspace) filled with 5 mM sodium phosphate buffer containing 100 μM DTPA at pH 7.4. The same amount of HCl was added before the addition of Proli/NO base solution to keep the pH at 7.4. For GSH or captopril nitrosation experiments, Proli/NO (final concentration of 1 μM $\cdot\text{NO}$) was added to 5 mM phosphate buffer containing 1 mM GSH or captopril \pm hydrophobic phases (Triton X-100, DLPC, and LDL), and the reaction was allowed to proceed for 5 min. *N*-ethylmaleimide (NEM)-modified LDL was prepared by incubating LDL (50 mg/mL) with 50 mM NEM for 30 min to alkylate all free thiols, followed by filtration with a 100 kDa cutoff filter to remove excess NEM. LDL modifications with high concentrations of $\cdot\text{NO}$ were performed in 10 mM phosphate buffer using 1 μM LDL exposed to 500 μM $\cdot\text{NO}$ from Proli/NO for 30 min at 37 $^\circ\text{C}$. All samples were treated with 40 mM NEM for 5 min, followed by 0.5% sulfanilamide \pm 0.2% HgCl_2 treatment for 15 min, and finally assayed by chemiluminescence (CLD 88 sp, ECO MEDICS). Oxymyoglobin (6 μM) was added to the sample to scavenge residual $\cdot\text{NO}$ immediately prior to chemiluminescence detection.

Results

Acceleration of $\cdot\text{NO}$ Disappearance by LDL, Membranes, and Micelles. The ability of LDL to accelerate $\cdot\text{NO}$ disappear-

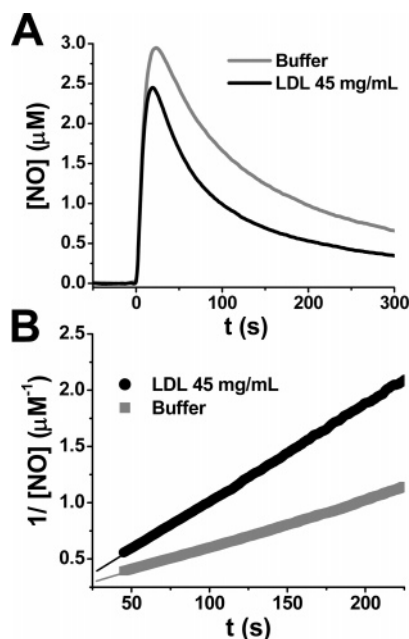


Figure 1. (A) $\cdot\text{NO}$ disappearance followed electrochemically after injecting $3.7 \mu\text{M}$ $\cdot\text{NO}$ (using Proli/NO) into a well-stirred, capped vessel with and without 45 mg/mL LDL (240 μM O_2 , 5 mM phosphate buffer, 100 μM DTPA, pH 7.4, 25 $^\circ\text{C}$). (B) Second-order linear transformation of $\cdot\text{NO}$ decay, which shows more clearly the higher rate of $\cdot\text{NO}$ disappearance in the presence of LDL. In both cases, there is a good fit, which indicates that this reaction depends on $[\cdot\text{NO}]^2$, in agreement with $\cdot\text{NO}$ autooxidation. For control conditions, it was found that $4k = 1.7 \times 10^7 \text{ M}^{-2} \text{ s}^{-1}$ (eq 7), whereas after adding LDL $4k = 3.6 \times 10^7 \text{ M}^{-2} \text{ s}^{-1}$.

ance was polarographically studied as previously described (16), except by using a different electrode, lower $\cdot\text{NO}$ concentrations, and delivering $\cdot\text{NO}$ from an $\cdot\text{NO}$ donor rather than from a stock $\cdot\text{NO}$ solution. It has been shown that adding $\cdot\text{NO}$ as a bolus from a concentrated solution may lead to heterogeneous $\cdot\text{NO}$ oxidation due to the high local $\cdot\text{NO}$ concentration at the tip of the syringe (26, 27). To overcome this possible bolus effect, we used Proli/NO, an $\cdot\text{NO}$ donor that has a very short half-life and readily yields $\cdot\text{NO}$ at neutral pH (28). Another important difference with previous works was the use of low concentrations of buffer salts, never greater than 10 mM, because phosphate inhibits nitrosation (4).

Figure 1A shows that LDL enhances the rate of $\cdot\text{NO}$ disappearance, and this difference in rate is more clearly demonstrated after a second-order linear transformation (Figure 1B). The good linearity confirmed that the disappearance of $\cdot\text{NO}$ was due to a second-order reaction for $\cdot\text{NO}$ and thus is consistent with autooxidation. In the presence of 45 mg/mL LDL, the rate of $\cdot\text{NO}$ autooxidation (k_{obs}) was 2.1 times larger than that in buffer (Figure 1B). The increase in $\cdot\text{NO}$ autooxidation rate ($k_{\text{obs}}^{\text{h}}/k_{\text{obs}}^{\text{control}}$) per mg/mL of the hydrophobic phase (LDL, lipid membranes, and Triton micelles) was determined as previously described (16) using eq 8

$$k_{\text{obs}}^{\text{h}}/k_{\text{obs}}^{\text{control}} = 1 + C_{\text{h}}\bar{v}_{\text{h}}\lambda \quad (8)$$

where \bar{v}_{h} is the partial specific volume, C_{h} the hydrophobic phase concentration (thus, $C_{\text{h}}\bar{v}_{\text{h}}$ is the fraction of the hydrophobic volume $V_{\text{h}}/V_{\text{Tot}}$), and λ is the acceleration coefficient on a per volume basis. The λ indicates how much faster $\cdot\text{NO}$ autooxidation occurs within the interior of a membrane relative to an equal volume of buffer (16). The slope of a plot of $k_{\text{obs}}^{\text{h}}/k_{\text{obs}}^{\text{control}}$ vs C_{h} will thus yield $\bar{v}_{\text{h}}\lambda$ (Figure 2). Because \bar{v}_{h} values are known for the assayed hydrophobic phases, the acceleration coefficients

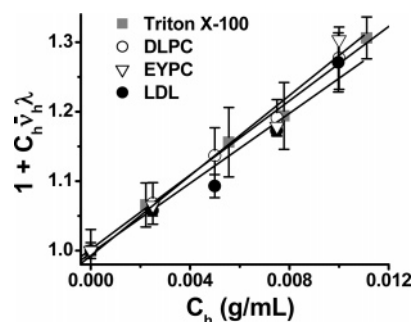


Figure 2. Increase in $\cdot\text{NO}$ autooxidation rate by different hydrophobic phases correlated with the concentration of the added hydrophobic phase (eq 8). The slope of this plot yields $\bar{v}_{\text{h}}\lambda$, which indicates how much the reaction is accelerated per g/mL. Because the \bar{v}_{h} values are known for the different hydrophobic phases (Table 1), the acceleration factors on a per volume basis can be calculated: $\lambda = 24 \pm 3$, 27 ± 3 , 28 ± 3 , and 30 ± 3 for LDL, DLPC, and EYPC liposomes and Triton X-100 micelles, respectively.

λ were obtained (Table 1). It was found that $\cdot\text{NO}$ autooxidation was accelerated to a similar extent by the different hydrophobic phases, $\lambda = 27 \pm 3$, 28 ± 3 , 30 ± 3 , and 24 ± 3 for DLPC liposomes, EYPC liposomes, Triton X-100 micelles, and LDL, respectively (Table 1). The $\cdot\text{NO}$ decayed by a similar mechanism in both aqueous and hydrophobic phases because the yield of nitrite relative to nitrite plus nitrate was $93 \pm 3\%$ in buffer and $90 \pm 1\%$ in 100 mg/mL Triton X-100.

Effect of LDL and Membranes on the Rate of $\cdot\text{NO}_2$ Formation. To confirm the observed results with the $\cdot\text{NO}$ electrode, the formation of $\cdot\text{NO}_2$ was studied by stopped-flow spectrophotometry using ABTS as a probe (1). A significant increase in the initial rate of ABTS oxidation is observed after the addition of either LDL or DLPC liposomes (Figure 3 A and B). The ratio between the ABTS oxidation rates was used to calculate λ for $\cdot\text{NO}_2$ formation using eq 8, and it was found that $\lambda = 17 \pm 4$, 20 ± 5 , and 31 ± 7 for LDL, EYPC, and DLPC, respectively, in good agreement with the polarographic results (Table 1). It should be noted that unlike DLPC or EYPC liposomes, LDL and Triton X-100 micelles displayed interference in the ABTS assay. Both LDL and Triton X-100 reacted with $\text{ABTS}^{+\cdot}$ and caused artifacts in the measurements. In fact, it was found that LDL rapidly reacts with $\text{ABTS}^{+\cdot}$ ($-\text{d}[\text{ABTS}^{+\cdot}]/\text{d}t = k[\text{ABTS}^{+\cdot}][\text{LDL}]$; $k \sim 9 \times 10^5 \text{ M}^{-1} \text{ s}^{-1}$). This effect was successfully bypassed by treating LDL with preformed $\text{ABTS}^{+\cdot}$ before the kinetic assay, but no solution was found for Triton X-100 micelles.

Acceleration of Thiol Nitrosation by LDL, Membranes, and Micelles. The effect of adding hydrophobic particles on thiol nitrosation kinetics was evaluated using captopril (Cap) and glutathione (GSH). When reacting 1 mM of each thiol (RSH) with 1 μM $\cdot\text{NO}$, approximately 100 nM *S*-nitrosothiol (RSNO) is detected by chemiluminescence after 5 min of reaction (Figure 4A). Because the half-life of 1 μM $\cdot\text{NO}$ in buffer is approximately 6 min (with the lifetime increasing with time), results from a 5 min time point reflect the rate rather than the total yield of reaction. Figure 4A shows that both DLPC (30 mg/mL) and Triton X-100 (100 mg/mL) significantly increase the formation of RSNO. No Hg^{2+} -resistant signal was found, indicating that only *S*-nitrosothiols are formed. LDL also accelerates GSH nitrosation, but this is evident only after blocking LDL intrinsic thiols with NEM (Figure 4B). Of note, LDL itself is *S*-nitrosated when studied in the absence of GSH. These results demonstrate that simple and complex hydrophobic phases can significantly accelerate the nitrosation of thiols.

Table 1. Comparison between Experimental and Theoretical Acceleration Coefficients^a

hydrophobic phase	$\bar{v}_h \lambda^{EC}$ (mL/g)	$\bar{v}_h \lambda^{SF}$ (mL/g)	\bar{v}_h (mL/g)	λ^{EC}	λ^{SF}	$K_p^{O_2}$	K_p^{NO}	λ^{theor} $K_p^{O_2}(K_p^{NO})^2$
LDL	23 ± 3	16 ± 4	0.96 ^b	24	17	2.6 ± 0.3 ^c	3.0 ± 0.4 ^c	24 ± 8
EYPC	28 ± 3	20 ± 5	0.983 ^b	28	20	3.2 ± 0.3 ^c	3.6 ± 0.3 ^c	40 ± 11
DLPC	26 ± 3	30 ± 7	0.962 ^b	27	31	3.2 ^d	3.6 ± 0.6	42 ± 17
Triton X-100	27 ± 3	ND	0.91 ^b	30	ND	2.6 ^d	3.1 ± 0.5	25 ± 10

^a The acceleration coefficient of $\cdot NO$ autoxidation (λ) was determined electrochemically (EC) or by stopped-flow spectrophotometry (SF) following ABTS oxidation or calculated (theor) from the partition coefficients. ^b Data from refs 29, 30, and 31, respectively. ^c Data corrected from ref 20 (see Materials and Methods). ^d Estimated as $0.85 \times K_p^{NO}$ (20).

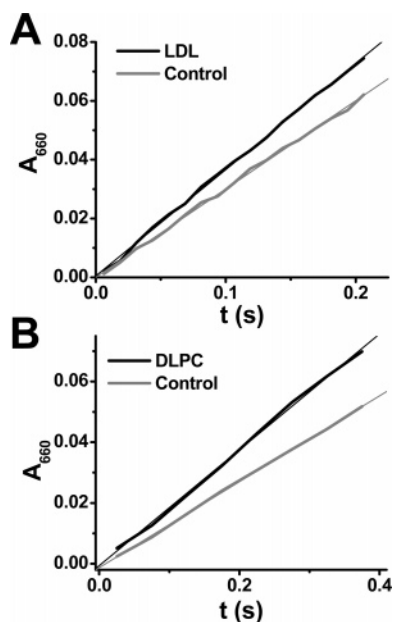


Figure 3. Formation of $\cdot NO_2$ studied by stopped-flow spectrophotometry following the initial rate of ABTS oxidation after $\cdot NO$ and O_2 mixing (1.5 mM phosphate buffer, 100 μM DTPA, pH 7.4, 120 μM O_2 , 1 mM ABTS final concentration and either 300 or 150 μM $\cdot NO$, 25 $^\circ C$, $n = 10$). (A) Representative trace of ABTS oxidation with and without LDL (9.1 mg/mL); (B) the same for DLPC liposomes (10 mg/mL). The higher rates of ABTS oxidation in the presence of the hydrophobic phase indicate higher rates of $\cdot NO_2$ formation, which correspond to an acceleration $\lambda = 17$ and 31 within LDL and DLPC liposomes, respectively.

LDL Modification by $\cdot NO/O_2$ Reactive Species. Because $\cdot NO$ autoxidation within LDL leads to a higher rate of formation of oxidizing and nitrosating species, potential modifications of this lipoprotein exposed to $\cdot NO/O_2$ were investigated. An important modification was described above, where LDL exposed to 1 μM $\cdot NO$ was found to be *S*-nitrosated (Figure 4B). In order to quantitatively determine the most important target of $\cdot NO/O_2$ species, LDL was exposed to higher $\cdot NO$ concentrations. Considering that LDL contains many unsaturated fatty acids that are susceptible to oxidation (21), lipid oxidation by $\cdot NO/O_2$ was investigated by following oxidation of the main lipid-soluble antioxidant α -tocopherol. When 1 μM LDL is exposed to 750 μM $\cdot NO$ in the presence of O_2 , the $2e^-$ -oxidation product of α -tocopherol, α -tocopherylquinone, accumulates up to 7%. Consistent with this mild lipid oxidation, no fluorescent lipid fragmentation products are observed by fluorimetry. In the protein component of LDL, no significant tryptophan oxidation/nitrosation is observed by fluorescence loss. However, LDL thiols are highly nitrosated, up to 34% (340 nM RSNO in 1 μM LDL). The high proportion of *S*-nitrosation is in agreement with the reactivity of the different components of LDL predicted by kinetics, in which thiols are the most reactive, even though they are present in low amounts (32). Noticeably, a significant fraction of the LDL chemiluminescence signal is Hg^{2+} -resistant,

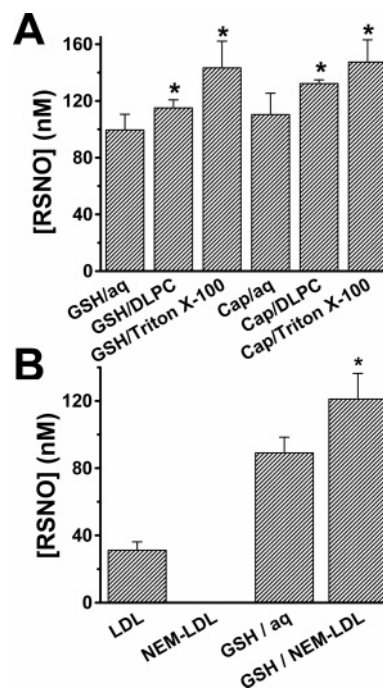
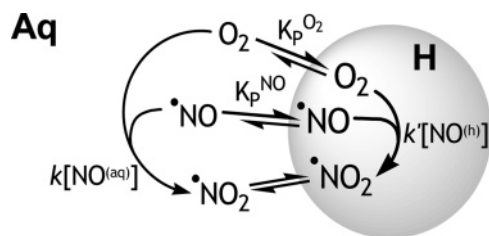


Figure 4. Influence of hydrophobic phases on thiol nitrosation assessed by measuring *S*-nitrosothiols formed 5 min after injecting 1 μM $\cdot NO$ (from Proli/NO). (A) $\cdot NO$ was injected into solutions containing 1 mM GSH or captopril (cap) in either aerated buffer, 30 mg/mL DLPC, or 100 mg/mL Triton X-100, and the higher formation of RSNO in the presence of the hydrophobic phase reflects a higher rate of nitrosation. (B) LDL (50 mg/mL) exposed to 1 μM $\cdot NO$ (from Proli/NO) for 5 min was found to be *S*-nitrosated, and this modification was prevented by treatment with 50 mM NEM. When 1 mM GSH was exposed to 1 μM $\cdot NO$, NEM-treated LDL significantly enhanced GSH *S*-nitrosation. The values represent the means \pm SD ($n = 4-6$; *, $p < 0.05$ compared with values in buffer). These reactions were performed in 5 mM sodium phosphate and 100 μM DTPA at pH 7.4 and room temperature.

which accounts for nearly 20% of the total LDL, resulting in the second most important modification in the particle. The Hg^{2+} -resistant fraction may well be due to tryptophan *N*-nitrosation, and this would not be detected by tryptophan fluorescence loss because it would represent only 0.5% tryptophan/LDL (37 tryptophanyl residues/LDL).

Discussion

In this work, we confirmed that the reaction between $\cdot NO$ and O_2 is accelerated approximately 30 times within hydrophobic compartments and demonstrated for the first time the accelerated formation of $\cdot NO_2$ as well as the more rapid nitrosation of thiols. At present, we have no definitive explanation for the discrepancy between the previously reported acceleration factor of 300 (16) and the value found here of 30. We note that there are several critical differences between these two studies: the higher $\cdot NO$ concentration used previously (30 μM compared to 3 μM), different electrodes, and bolus

Scheme 1. Membrane "Lens" Effect in $\cdot\text{NO}$ Autooxidation^a

^a This scheme shows different factors that may account for the observed acceleration in $\cdot\text{NO}$ autooxidation by hydrophobic phases: the higher solubility of $\cdot\text{NO}$ and O_2 into the hydrophobic phase (H) relative to the aqueous phase (Aq), characterized by the partition coefficients K_p , and the possible differences in the intrinsic rate constant for $\cdot\text{NO}$ autooxidation (eq 7) in the aqueous (k) or hydrophobic phases (k'). The solubility of $\cdot\text{NO}_2$ in membranes is not known, but the equilibrium indicates that all these species can easily and rapidly diffuse in and out of biological hydrophobic phases. The formation of N_2O_3 was omitted for clarity.

compared to rapid-donor addition of $\cdot\text{NO}$. Nevertheless, we are confident that the acceleration coefficient value reported here is correct because the same value of around 30 was obtained by different experimental approaches (Table 1).

The increase in $\cdot\text{NO}$ autooxidation rate by hydrophobic phases could be explained by the following: (1) the increase in concentration of both $\cdot\text{NO}$ and O_2 within the membrane, given by the corresponding partition coefficients K_p^{NO} and $K_p^{\text{O}_2}$; and/or (2) an increase in the intrinsic rate constant within the hydrophobic phase (k') relative to the aqueous phase (k) (Scheme 1). Thus, the acceleration coefficient λ is defined as follows (16):

$$\lambda = K_p^{\text{O}_2} (K_p^{\text{NO}})^2 k'/k \quad (9)$$

If we calculate a theoretical acceleration coefficient λ using just the experimentally determined K_p values (20), good agreement is found between the theoretical and the experimental λ values (Table 1), indicating that the acceleration of $\cdot\text{NO}$ autooxidation in hydrophobic structures is mainly due to a solubility effect. Furthermore, neither polarity nor viscosity are expected to affect the intrinsic rate constant, that is, $k \cong k'$, because (a) $\cdot\text{NO}$ reacts with O_2 in a nonpolar solvent (carbon tetrachloride) with the same rate constant as in water ($k = 2.8 \times 10^6 \text{ M}^{-2} \text{ s}^{-1}$, ref 3, vs $3 \times 10^6 \text{ M}^{-2} \text{ s}^{-1}$ in aqueous media, ref 1), and (b) this is not a diffusion-controlled reaction; therefore, no effect is expected from the ~ 10 times slower diffusion of $\cdot\text{NO}$ and O_2 in LDL or membranes relative to the aqueous phase (20, 33). Therefore, the results support a "lens effect": the higher solubility of both $\cdot\text{NO}$ and O_2 in the hydrophobic phase leads to a higher local concentration, a focusing of reactants, which results in a higher rate of reaction (Scheme 1). A useful outcome of this observation is that a good estimate of K_p^{NO} values may be obtained from $\cdot\text{NO}$ autooxidation assays. In any given system where λ is easier to determine than K_p^{NO} , the experimental λ value can be used to calculate an approximate K_p^{NO} : $K_p^{\text{NO}} \approx (\lambda)^{1/3}$, considering that K_p^{NO} is similar to $K_p^{\text{O}_2}$ (Table 1 and ref 20).

In a biological milieu, this acceleration of $\cdot\text{NO}$ autooxidation may be of essentially no consequence with regard to $\cdot\text{NO}$ disappearance because there are more rapid reactions that remove $\cdot\text{NO}$ (34). However, it could be important in terms of producing highly reactive species because hydrophobic compartments become sites of enhanced $\cdot\text{NO}_2$ and N_2O_3 production (Figures 3 and 4). In the case of LDL, these reactive species react mainly with the thiols of the apolipoprotein B-100. There are nine free cysteinyl residues in apolipoprotein B-100, mostly

located in hydrophobic environments (32, 35). The selectivity of reactive nitrogen species for thiols reflects their high reactivity, also evidenced by their important activity as inhibitors of LDL lipid peroxidation (36). The mild modification of LDL by this oxidizing system and the absence of cysteinyl residues at the LDL receptor binding domain (site B, residues 3359–3367, ref 37) suggest that it should not be a deleterious modification that affects LDL uptake by cells or leads to a proatherogenic particle, supporting previous results (38).

This accelerated $\cdot\text{NO}$ autooxidation is probably more important in cell membranes than in circulating LDL because membranes are exposed to higher levels of $\cdot\text{NO}$. In fact, up to 500 nM $\cdot\text{NO}$ has been detected in stimulated endothelial cells (39). Considering a lower steady-state concentration of 100 nM $\cdot\text{NO}$, 50 μM O_2 , and the acceleration factor of 30 determined here, the rate of intramembrane $\cdot\text{NO}_2$ (and possibly N_2O_3) formation will be $\sim 3.6 \text{ nM/min}$, a rate capable of causing substantial amounts of nitrosation. Cellular S-nitrosation resembles $\cdot\text{NO}$ autooxidation because it is a very inefficient process (40) that sharply increases after $\cdot\text{NO}$ concentration is raised by iNOS induction (40, 41).

Furthermore, if membranes account for 3% of the cellular volume and $\cdot\text{NO}$ autooxidation is accelerated ~ 30 times, we can estimate that 50% of this reaction will occur in the membranes. Therefore, half of the $\cdot\text{NO}_2$ and N_2O_3 derived from $\cdot\text{NO}$ autooxidation will be produced inside membranes and, importantly, in a very small volume. Membranes and membrane-associated proteins will then be exposed to approximately 30-fold higher fluxes of oxidizing and nitrosating species than cytosolic targets. In fact, several membrane proteins have been identified as targets of nitrosation, such as the NMDA receptor, the ryanodine receptor, the olfactory cyclic-nucleotide-gated channel, and eNOS (7, 8). However, even if the concentrations and fluxes of $\cdot\text{NO}$, $\cdot\text{NO}_2$, and N_2O_3 are higher near the membrane, we should not forget that these species are diffusible and could travel significant distances from the source, depending on the concentration and reactivity of substrates. For instance, in the presence of 5 mM GSH, the half-life of $\cdot\text{NO}_2$ is 7 μs , enough to travel 200 nm, 40 times the thickness of a membrane (42, 43). Therefore, membranes catalyze the formation but may not confine the reactivity of these oxidizing and nitrosating species to the membrane per se.

In summary, we provide here novel quantitative and mechanistic information about the acceleration of $\cdot\text{NO}$ autooxidation and the formation of derived reactive species by lipoproteins and membranes that may aid in the understanding of the formation and function of biological nitrosation products as well as a basis to explore other routes of biological nitrosation (6, 7).

Acknowledgment. We thank Horacio Botti, Gerardo Ferrer-Sueta, and Rafael Radi for helpful discussions and collaboration. This work was supported in part by grants TW007357 from the NIH (to J.R.L. and A.D.), HL074391 (to J.R.L.), and C.S.I.C., Uruguay (to A.D.). M.N.M. and D.A.V. were partially supported by fellowships from PEDECIBA and C.S.I.C., Uruguay, respectively.

References

- (1) Goldstein, S., and Czapski, G. (1995) Kinetics of nitric oxide autooxidation in aqueous solution in the absence and presence of various reductants. The nature of the oxidizing intermediates, *J. Am. Chem. Soc.* 117, 12078–12084.
- (2) Goldstein, S., and Czapski, G. (1996) Mechanism of the nitrosation of thiols and amines by oxygenated NO solutions: the nature of the nitrosating intermediates, *J. Am. Chem. Soc.* 118, 3419–3425.
- (3) Nottingham, W. C., and Sutter, J. R. (1986) Kinetics of the oxidation of nitric oxide by chlorine and oxygen in nonaqueous media, *Int. J. Chem. Kinet.* 18, 1289–1302.

- (4) Lewis, R. S., Tannenbaum, S. R., and Deen, W. M. (1995) Kinetics of N-nitrosation in oxygenated nitric oxide solutions at physiological pH: role of nitrous anhydride and effects of phosphate and chloride, *J. Am. Chem. Soc.* **117**, 3933–3939.
- (5) Hogg, N. (2002) The biochemistry and physiology of S-nitrosothiols, *Annu. Rev. Pharmacol. Toxicol.* **42**, 585–600.
- (6) Jourdain, D., Jourdain, F. L., and Feelisch, M. (2003) Oxidation and nitrosation of thiols at low micromolar exposure to nitric oxide. Evidence for a free radical mechanism, *J. Biol. Chem.* **278**, 15720–15726.
- (7) Hess, D. T., Matsumoto, A., Kim, S. O., Marshall, H. E., and Stamler, J. S. (2005) Protein S-nitrosylation: purview and parameters, *Nat. Rev. Mol. Cell Biol.* **6**, 150–166.
- (8) Erwin, P. A., Mitchell, D. A., Sartoretto, J., Marletta, M. A., and Michel, T. (2006) Subcellular targeting and differential S-nitrosylation of endothelial nitric-oxide synthase, *J. Biol. Chem.* **281**, 151–157.
- (9) Morrell, C. N., Matsushita, K., Chiles, K., Scharpf, R. B., Yamakuchi, M., Mason, R. J., Bergmeier, W., Mankowski, J. L., Baldwin, W. M., III, Faraday, N., and Lowenstein, C. J. (2005) Regulation of platelet granule exocytosis by S-nitrosylation, *Proc. Natl. Acad. Sci. U.S.A.* **102**, 3782–3787.
- (10) Hara, M. R., Agrawal, N., Kim, S. F., Cascio, M. B., Fujimuro, M., Ozeki, Y., Takahashi, M., Cheah, J. H., Tankou, S. K., Hester, L. D., Ferris, C. D., Hayward, S. D., Snyder, S. H., and Sawa, A. (2005) S-nitrosylated GAPDH initiates apoptotic cell death by nuclear translocation following Siah1 binding, *Nat. Cell Biol.* **7**, 665–674.
- (11) Yao, D., Gu, Z., Nakamura, T., Shi, Z. Q., Ma, Y., Gaston, B., Palmer, L. A., Rockenstein, E. M., Zhang, Z., Masliah, E., Uehara, T., and Lipton, S. A. (2004) Nitrosative stress linked to sporadic Parkinson's disease: S-nitrosylation of parkin regulates its E3 ubiquitin ligase activity, *Proc. Natl. Acad. Sci. U.S.A.* **101**, 10810–10814.
- (12) Schonhoff, C. M., Matsuoka, M., Tummala, H., Johnson, M. A., Estevez, A. G., Wu, R., Kamaid, A., Ricart, K. C., Hashimoto, Y., Gaston, B., Macdonald, T. L., Xu, Z., and Mannick, J. B. (2006) S-nitrosothiol depletion in amyotrophic lateral sclerosis, *Proc. Natl. Acad. Sci. U.S.A.* **103**, 2404–2409.
- (13) Dedon, P. C., and Tannenbaum, S. R. (2004) Reactive nitrogen species in the chemical biology of inflammation, *Arch. Biochem. Biophys.* **423**, 12–22.
- (14) Baker, P. R., Schopfer, F. J., Sweeney, S., and Freeman, B. A. (2004) Red cell membrane and plasma linoleic acid nitration products: synthesis, clinical identification, and quantitation, *Proc. Natl. Acad. Sci. U.S.A.* **101**, 11577–11582.
- (15) Wright, M. M., Schopfer, F. J., Baker, P. R., Vidyasagar, V., Powell, P., Chumley, P., Iles, K. E., Freeman, B. A., and Agarwal, A. (2006) Fatty acid transduction of nitric oxide signaling: nitrooleic acid potentially activates endothelial heme oxygenase 1 expression, *Proc. Natl. Acad. Sci. U.S.A.* **103**, 4299–4304.
- (16) Liu, X., Miller, M. J., Joshi, M. S., Thomas, D. D., and Lancaster, J. R., Jr. (1998) Accelerated reaction of nitric oxide with O₂ within the hydrophobic interior of biological membranes, *Proc. Natl. Acad. Sci. U.S.A.* **95**, 2175–2179.
- (17) Möller, M. N., Li, Q., Lancaster, J. R., Jr., and Denicola, A. (2007) Accelerated nitric oxide autooxidation and nitrosation in membranes, *IUBMB Life*, in press.
- (18) Steinberg, D. (1997) Low density lipoprotein oxidation and its pathobiological significance, *J. Biol. Chem.* **272**, 20963–20966.
- (19) Denicola, A., Batthyany, C., Lissi, E., Freeman, B. A., Rubbo, H., and Radi, R. (2002) Diffusion of nitric oxide into low density lipoprotein, *J. Biol. Chem.* **277**, 932–936.
- (20) Möller, M., Botti, H., Batthyany, C., Rubbo, H., Radi, R., and Denicola, A. (2005) Direct measurement of nitric oxide and oxygen partitioning into liposomes and low density lipoprotein, *J. Biol. Chem.* **280**, 8850–8854.
- (21) Esterbauer, H., Gebicki, J., Puhl, H., and G. J. (1992) The role of lipid peroxidation and antioxidants in oxidative modification in LDL, *Free Radical Biol. Med.* **13**, 341–390.
- (22) Forni, L. G., Mora-Arellano, V. O., Packer, J. E., and Willson, R. L. (1986) Nitrogen dioxide and related free radicals: electron-transfer reactions with organic compounds in solutions containing nitrite or nitrate, *J. Chem. Soc., Perkin Trans. 2* **1**, 1–6.
- (23) Botti, H., Batthyany, C., Trostchansky, A., Radi, R., Freeman, B. A., and Rubbo, H. (2004) Peroxynitrite-mediated alpha-tocopherol oxidation in low-density lipoprotein: a mechanistic approach, *Free Radical Biol. Med.* **36**, 152–162.
- (24) Trostchansky, A., Batthyany, C., Botti, H., Radi, R., Denicola, A., and Rubbo, H. (2001) Formation of lipid-protein adducts in low-density lipoprotein by fluxes of peroxynitrite and its inhibition by nitric oxide, *Arch. Biochem. Biophys.* **395**, 225–232.
- (25) Wang, X., Bryan, N. S., MacArthur, P. H., Rodriguez, J., Gladwin, M. T., and Feelisch, M. (2006) Measurement of nitric oxide levels in the red cell: validation of tri-iodide-based chemiluminescence with acid-sulfanilamide pretreatment, *J. Biol. Chem.* **281**, 26994–27002.
- (26) Zhang, Y., and Hogg, N. (2002) Mixing artifacts from the bolus addition of nitric oxide to oxymyoglobin: implications for S-nitrosothiol formation, *Free Radical Biol. Med.* **32**, 1212–1219.
- (27) Joshi, M. S., Ferguson, T. B., Jr., Han, T. H., Hyduke, D. R., Liao, J. C., Rassaf, T., Bryan, N., Feelisch, M., and Lancaster, J. R., Jr. (2002) Nitric oxide is consumed, rather than conserved, by reaction with oxyhemoglobin under physiological conditions, *Proc. Natl. Acad. Sci. U.S.A.* **99**, 10341–10346.
- (28) Saavedra, J. E., Southan, G. J., Davies, K. M., Lundell, A., Markou, C., Hanson, S. R., Adrie, C., Hurford, W. E., Zapol, W. M., and Keefer, L. K. (1996) Localizing antithrombotic and vasodilatory activity with a novel, ultrafast nitric oxide donor, *J. Med. Chem.* **39**, 4361–4365.
- (29) White, S. H., Jacobs, R. E., and King, G. I. (1987) Partial specific volumes of lipid and water in mixtures of egg lecithin and water, *Biophys. J.* **52**, 663–665.
- (30) Balgavy, P., Dubnickova, M., Kucerka, N., Kiselev, M. A., Yaradaikin, S. P., and Uhrkova, D. (2001) Bilayer thickness and lipid interface area in unilamellar extruded 1,2-diacetylphosphatidylcholine liposomes: a small-angle neutron scattering study, *Biochim. Biophys. Acta* **1512**, 40–52.
- (31) Robson, R., and Dennis, E. (1977) The size, shape, and hydration of nonionic surfactant micelles. Triton X-100, *J. Phys. Chem.* **81**, 1075–1078.
- (32) Kveder, M., Krisko, A., Pifat, G., and Steinhoff, H.-J. (2003) The study of structural accessibility of free thiol groups in human low-density lipoprotein, *Biochim. Biophys. Acta* **1631**, 239–245.
- (33) Eigen, M. (1967) Proton transfer and general acid base catalysis. Fast reactions and primary processes in chemical kinetics, *Nobel Symp.* **5**, 245–253.
- (34) Thomas, D. D., Liu, X., Kantrow, S. P., and Lancaster, J. R., Jr. (2001) The biological lifetime of nitric oxide: implications for the perivascular dynamics of NO and O₂, *Proc. Natl. Acad. Sci. U.S.A.* **98**, 355–360.
- (35) Singh, R. J., Feix, J. B., Mchaourab, H. S., Hogg, N., and Kalyanaram, B. (1995) Spin-labeling study of the oxidative damage to low-density lipoprotein, *Arch. Biochem. Biophys.* **320**, 155–161.
- (36) Ferguson, E., Singh, R. J., and Kalyanaram, B. (1997) The mechanism of apolipoprotein B-100 thiol depletion during oxidative modification of low density lipoprotein, *Arch. Biochem. Biophys.* **341**, 287–294.
- (37) Segrest, J. P., Jones, M. K., De, Loof, H., and Dashti, N. (2001) Structure of apolipoprotein B-100 in low density lipoproteins, *J. Lipid Res.* **42**, 1346–1367.
- (38) Jessup, W., Mohr, D., Gieseg, S. P., Dean, R. T., and Stocker, R. (1992) The participation of nitric oxide in cell free- and its restriction of macrophage-mediated oxidation of low-density lipoprotein, *Biochim. Biophys. Acta* **1180**, 73–82.
- (39) Wadsworth, R., Stankevicius, E., and Simonsen, U. (2006) Physiologically relevant measurements of nitric oxide in cardiovascular research using electrochemical microsensors, *J. Vasc. Res.* **43**, 70–85.
- (40) Zhang, Y., and Hogg, N. (2004) Formation and stability of S-nitrosothiols in RAW 264.7 cells, *Am. J. Physiol.: Lung Cell. Mol. Physiol.* **287**, L467–L474.
- (41) Jourdain, D., Gray, L., and Grisham, M. B. (2000) S-nitrosothiol formation in blood of lipopolysaccharide-treated rats, *Biochem. Biophys. Res. Commun.* **273**, 22–26.
- (42) Ford, E., Hughes, M. N., and Wardman, P. (2002) Kinetics of the reactions of nitrogen dioxide with glutathione, cysteine, and uric acid at physiological pH, *Free Radical Biol. Med.* **32**, 1314–1323.
- (43) Lancaster, J. R., and Jr. (1996) Diffusion of free nitric oxide, *Methods Enzymol.* **268**, 31–50.

TX700010H